Volume 1 | Number 1 | Jan 2013 | Pages 1–100

Nanoscale

www.rsc.org/nanoscale

ROYAL SOCIETY OF CHEMISTRY

This is an *Accepted Manuscript*, which has been through the Royal Society of Chemistry peer review process and has been accepted for publication.

Accepted Manuscripts are published online shortly after acceptance, before technical editing, formatting and proof reading. Using this free service, authors can make their results available to the community, in citable form, before we publish the edited article. We will replace this *Accepted Manuscript* with the edited and formatted *Advance Article* as soon as it is available.

You can find more information about *Accepted Manuscripts* in the **Information for Authors**.

Please note that technical editing may introduce minor changes to the text and/or graphics, which may alter content. The journal's standard **Terms & Conditions** and the **Ethical guidelines** still apply. In no event shall the Royal Society of Chemistry be held responsible for any errors or omissions in this *Accepted Manuscript* or any consequences arising from the use of any information it contains.

ROYAL SOCIETY OF CHEMISTRY

www.rsc.org/nanoscale

Nanoscale

PAPER

Preparation of Graphite Intercalation Compounds Containing Oligo and Polyethers

Hanyang Zhang[a] and Michael M. Lerner[a]

Layered host-polymer nanocomposites comprising polymeric guests between inorganic sheets have been prepared with many inorganic hosts, but there is limited evidence for the incorporation of polymeric guests into graphite. Here we report for the first time the preparation, and structural and compositional characterization of graphite intercalation compounds (GICs) containing polyether bilayers. The new GICs are obtained by either (1) reductive intercalation of graphite with an alkali metal in the presence of an oligo or polyether and an electrocatalyst, or (2) co-intercalate exchange of an amine for an oligo or polyether in a donor-type GIC. Structural characterization of products using powder X-ray diffraction, Raman spectroscopy, and thermal analyses support the formation of well-ordered, first-stage GICs containing alkali metal cations and oligo or polyether bilayers between reduced graphene sheets.

Introduction

Layered host-polymer nanocomposites have been prepared from many materials combinations[1] including the following hosts; layered smectite clays,[2] MO_2,[3] MS_2,[4] MoO_3[5] and MPS_3[6] and the polymeric guests that include polylactide,[7] poly(vinyl pyrrolidone),[6] linear poly(ethylenimine),[6] poly(vinyl alcohol),[8] and poly(ethylene oxide).[4,5,9] The resulting nanocomposites may be ordered, most often retaining co-planarity of inorganic host layers with intercalate galleries opened for the polymers, or they may be disordered, for example with delaminated inorganic nanosheets dispersed into a polymer matrix.[10] Because nanoscale composites often display significant property changes from both the native constituents and microscale composites,[11] they may be applied as enhanced structural materials, gas barriers, or thermal/fire resistant components.[12]

There are several synthetic approaches to generating nanocomposites,[1,13] including (1) intercalation of monomeric precursors followed by *in situ* polymerization,[14] (2) layered host exfoliation followed by sorption of polymer and reassembly of the nanocomposites (either in a solvent or as a solvent-free "melt-intercalation" process),[9] (3) direct topochemical intercalation of the polymer between host layers,[15] and (4) templated growth of the inorganic layers on the polymer.[6]

The nanoscale combination of polymers with graphite is a special case that presents significant challenges. Graphite has a high chemical potential for oxidation ($\approx$ 4.5-5.0 V vs Li(m)/Li$^+$)[16] and low chemical potential ($\approx$ 0.2-1.0 V vs Li(m)/Li$^+$) for reduction,[17] which significantly limits the number of stable intercalates and solvents. Furthermore, graphene sheet flexibility results in the unique stack ordering effect called staging,[18,19] which maintains a relatively constant graphene sheet charge density during intercalation.[20] This limits, perhaps closes, the possibility of effecting host delamination via redox titration. The template approach is of course unlikely to succeed with organic polymers given the high temperatures (>500°C) required to crack molecular precursors such as alkanes.

Still, there have been previous reports on forming graphite intercalation compounds containing polymeric guests. The donor-type graphite intercalation compounds (GICs) such as KC_8 are well known to function as polymerization catalysts, and can uptake polymerizable co-intercalates including ethylene,[21] styrene[22] and butadiene.[23] Shioyama *et al*[24] have reported the *in situ* polymerization of such vinyl co-intercalates. However, the products were highly disordered, precluding strong evidence for the nanocomposite structure. Additionally, the differentiation of bulk, surface-adsorbed and intercalated polymer remains a challenge for materials derived using this approach.[25]

Graphite oxide (GO) can be dispersed into polar solvents and thus undergo solution-phase processing.[26] GO has been shown to form nanocomposites with polyethers.[27] Related approaches have employed chemically and thermally

[a.] Department of Chemistry, Oregon State University, Corvallis, Oregon 97331, United States. Email: Michael.Lerner@oregonstate.edu

pretreated graphite (including thermally exfoliated graphites, graphenes, graphite oxide, or reduced graphene oxide) to generate nanocomposite materials with dispersed graphene nanosheets.[28]

Our group has recently explored the co-intercalation of linear and branched amines to form GICs with expanded and unusual intercalate conformations and arrangements.[29] Subsequent ion exchange can rapidly and quantitatively generate well-ordered GICs with intercalates as large as $(C_{18}H_{37})_2N(CH_3)_2^+$ (molar mass = 551 D).[30] This work suggested the plausibility for incorporating oligomeric or polymeric constituents via similar exchange reactions; and these exchange reaction products are characterized in this report. We also found, surprisingly, as described below, that the direct reductive intercalation of oligo and polyethers can lead to similar products. Polymer candidates must be reductively stable to <1.0 V vs Li(m)/Li$^+$. They should strongly solvate alkali metal cations to provide favourable energetics for co-intercalation. Poly(ethylene glycol) (PEG), and poly(ethylene oxide) (PEO) were selected as they are ether-group abundant and show M$^+$ binding constants linearly proportional to chain length;[31] both readily form nanocomposites with many layered hosts.[2,4-6,9] The methylated derivatives, poly(ethylene glycol) dimethyl ethers (PEGDME), $CH_3O(CH_2CH_2O)_nCH_3$, were used for lower molecular weight reagents to avoid reduction of terminal groups.

The co-intercalation of small molecular ethers with alkali metal cations to form GICs has been established; there are reports for (1) tetrahydrofuran (THF) and derivatives 2-methylTHF, 2,5-dimethylTHF;[32] (2) diethylether and *t*-butylmethyl ether;[33] (3) dialkoxymethanes and dialkoxyethanes;[33] (4) the macrocyclic 2.2.2-cryptand.[34] and (5) diglyme[35] and diethylene glycol dimethyl ether.[36] Most of these GICs were obtained by direct reduction of graphite by alkali metals in the ether solvent; some reactions used electrochemical reduction.

Experimental

Syntheses

Dimethoxyethane (dme, 99+%, Alfa-Aesar) and ethylenediamine (en, Alfa Aesar, 99%) were used as received. Glassware and graphite reagents were dried at 120 °C prior to use. PEGDMEs (Sigma-Aldrich) and PEG-6k (TCI America, PEG with M$_W$= 6,000) were dried overnight under dynamic vacuum (<10 μm). For direct reactions, 0.25 g (21 mmol) of graphite (SP-1 grade, Union Carbide Corp., 100 μm, or Synthetic, Aldrich, 1-2 μm) and 2.0 mL (for liquid) or 2.0 g (for solid) polymer were combined with 3.5 mmol of Li (Sigma-Aldrich, 99.9%), Na (Alfa Aesar, 99.95%), or K (Alfa Aesar, 99.5%) metal and a naphthalene or phenanthrene as electrocatalyst (≈5 mg) in sealed glass tube under N$_2$(g) (or under Ar(g) for Li(m) reactions). The reactions were maintained at 90°C for ≥20 h. For ion-exchange reactions, 0.25-1.0 g of polymer (as indicated below) and 0.25 g of graphite were added to en (1.0 g) and Na (0.10 g) in a sealed glass tube and stirred continuously under N$_2$ at 60°C for 20 h. Products were isolated using centrifugation and separation of the solid phase, and then dried under vacuum at 60°C for 6 h. Products were dried in inverted test tubes to allow most excess polymer to flow away from the samples.

Characterization

Powder X-ray diffraction (PXRD) patterns were acquired using a Rigaku Miniflex II diffractometer with Ni-filtered Cu Kα radiation (λ= 0.15406 nm). Samples were loaded in the drybox into air-tight sample holders. Data were collected in the 2θ range from 3-60° at 3°/min. One dimensional electron density maps were generated from PXRD data using a method described previously.[37] Domain sizes were derived from the modified Scherer relation.[38] A TA Q50 thermogravimetric analyzer (TGA) was employed using a heating rate of 10 °C/min under flowing N$_2$ (Ar for lithium products) or O$_2$, and first derivatives of thermal responses (dTGA) were calculated. Raman spectra (resolution≈4 cm^{-1}) were obtained with a Witech confocal Raman microscope equipped with a 514 nm laser source. Raman and TGA samples were exposed to ambient conditions for < 1 min.

Results and Discussions

The GIC products reported below were obtained using either (1) the direct reaction of graphite, polymer, alkali metal and an electrocatalyst above the polymer melting point, or (2) graphite, polymer, alkali metal in ethylenediamine (en).

PXRD structural studies

Using the larger particle SP-1 graphite, direct reaction products with PEGDME co-intercalate M$_W$ ≤ 1,000 were dark blue, those with M$_W$ > 1,000 were dull-black. PXRD data (Fig. 1a) show the product obtained with dme is a stage 1 GIC (stage *n* indicates that *n* graphene layers separate intercalates) with a basal repeat, d_i = 0.73 nm, corresponding to a gallery expansion of $\Delta d = d_i$ – 0.335 nm = 0.40 nm. This dimension agrees well with previous work, with cations and dme monolayers between graphene sheets.[39] Direct reaction products with the low molecular weight PEGDMEs (M$_W$ ≤ 500) show no identifiable new phases, but have weak and broadened graphite (002) peaks, indicating that bulk intercalation occurs but results in unstable products, leading to higher-stage GICs and/or disordered materials. In contrast, reaction with PEGDME-1k yields a well-ordered new phase with d_i = 1.164 nm. The corresponding gallery height, Δd = 0.83 nm, is similar those for PEO-containing nanocomposites with polymer bilayers in other inorganic hosts.[2,4,9] These suggest a structure model with single graphene sheets separated by bilayers containing Na$^+$ and PEGDME co-intercalate, confirmed by the observed 1D gallery electron density map.[37] (Fig. 2) The domain size obtained from PXRD peak widths (Table 1, also see ESI†) indicates ≈30 coherent stack repeats per domain. Reactions with PEGDME-2k and higher did not generate new GIC products with SP-1 graphite. However, a smaller particle size synthetic graphite (domain size ≈1-2 μm) reacts as above with PEG-6k to form a well-ordered GIC, again with Δd = 0.83 nm.

Nanoscale Accepted Manuscript
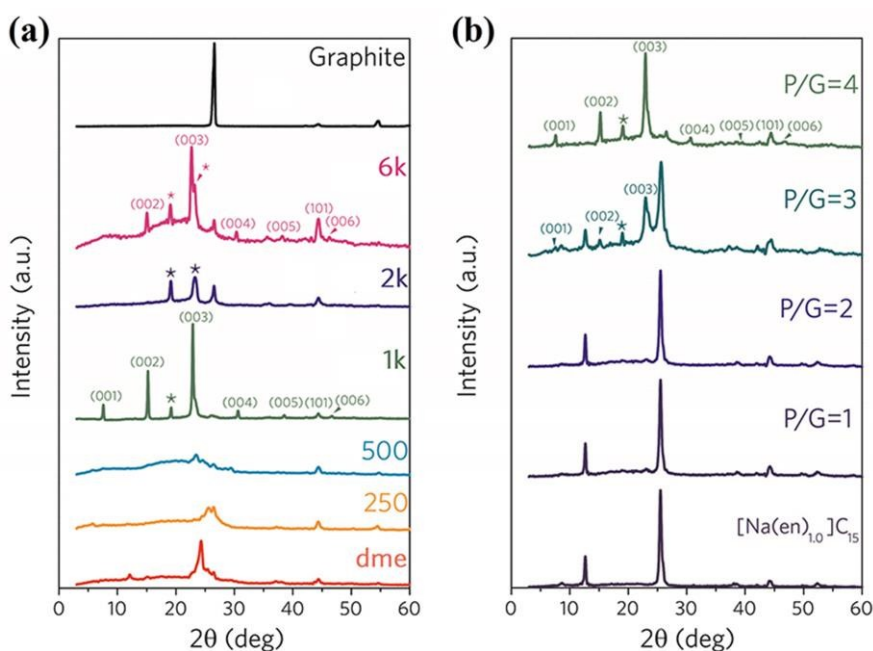
Fig. 1 *Ex situ* PXRD patterns for products of (a) direct reaction products, from bottom to top are graphite, Na(m), and either dimethoxyethane, PEGDMEs with M_W = 250-2k, or PEG-6k, and (b) exchange reaction products with PEGDME-2k and the polymer/graphite (P/G) ratios indicated. Asterisks (*) indicate native polymer phase peaks. Miller indices (*hkl*) are included only for peaks ascribed to new GIC products.
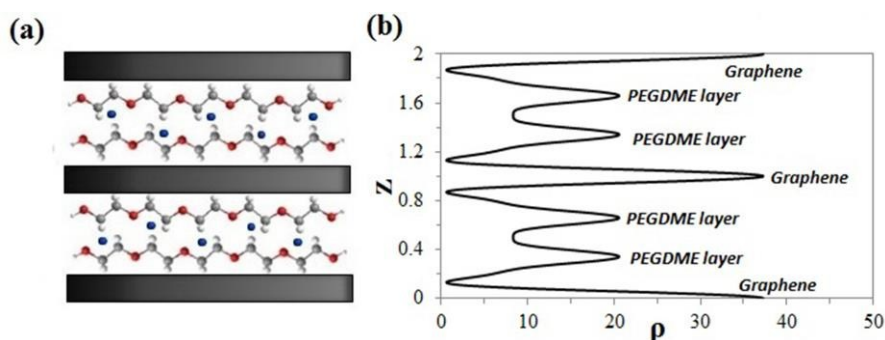
Fig 2 Schematic diagram of (a) M-PEG(DME)-GIC bilayer structure and (b) a 1D-electron density map generated from Na-PEGDME1k-GIC diffraction data showing the gallery bilayers.
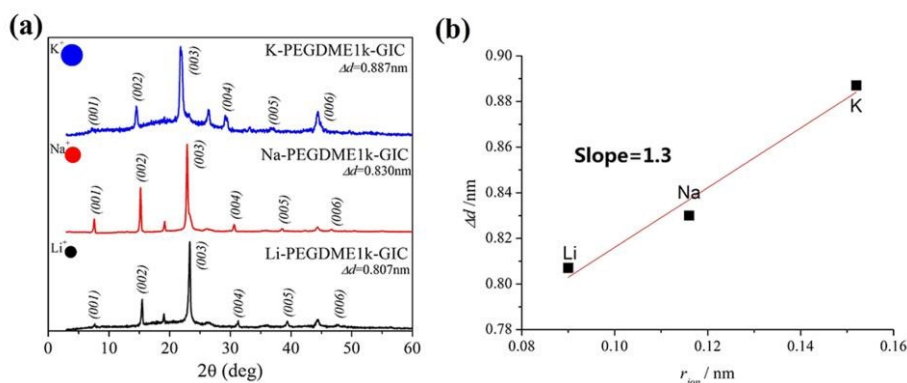
Fig. 3 (a) Ex situ PXRD patterns of direct reaction products using Li, Na or K metal and PEGDME-1k, and (b) gallery expansion for these GICs *vs.* ionic radii of the alkali cations.

The higher viscosity and lower diffusion rates for longer polymer chains are likely to create a kinetic restriction for direct intercalation of high Mw polymers; the dissolution of PEG into the electride solution may facilitate a more rapid reaction. The combination of en and alkali metals with graphite generates $[Na(en)_y]C_x$, so we hypothesize that $[Na(en)_y]C_x$ forms first and then PEG is exchanged for en.[29,30] so we hypothesized that this initial product will form and then might exchange PEG for the en co-intercalate.

The reaction of PEGDME-2k with SP-1 graphite at polymer/graphite ratios ≤2 generates only $[Na(en)_{1.0}]C_{15}$ (Fig. 1b). Increasing the polymer reagent content to P/G = 3, a new GIC phase appears, and at P/G = 4 only this new GIC phase and excess polymer are observed, indicating complete exchange of en for the polyether. The gallery expansion is, as before, $\Delta d = 0.83$ nm, and the sharp PXRD peaks again indicate a well-ordered GIC product.

Li, Na, and K reactions using the direct method with PEGDME-1k all generate new single phase GICs with a linear response of gallery expansion vs. alkali metal ionic radius (Fig. 3). The slope of this plot, ≈1.3, confirms that more than a single cation-containing layer contributes to the gallery expansion.

Raman study

Raman spectra are sensitive to graphene layer charge; donor-type GICs display an E_{2g} (G band) peak shift to higher wavenumber due to occupancy of in-plane antibonding orbitals. A 12-14 cm^{-1} shift has been reported for LiC_6.[40] Fig. 4 shows the G band peak for graphite at 1576 cm^{-1}, and for the GIC products at 1596-1601 cm^{-1}, indicating reduction of the graphene sheets. The low D/G band ratios obtained (See ESI†)
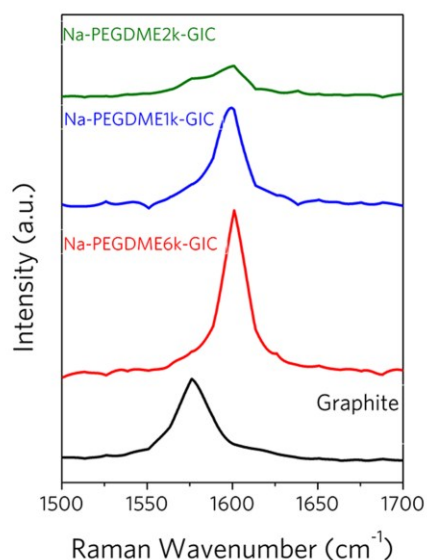

Fig. 4 Raman spectra show a G band peak at 1576 cm^{-1} for native graphite, with a blue shift to 1596-1601 cm^{-1} for GICs with PEGDMEs.

for graphite and the GIC products confirm that graphene sheets do not accumulate defects in these reactions.

Compositions using thermoanalysis

We employed a simple gravity separation method (allowing polymer to flow out of sample maintained at 60°C for 6 h) to remove excess polymer after reaction. Still, the products obtained are all admixtures of GICs with the polymer reagents. TGA and dTGA (Fig. 5) show two mass loss features in all GIC
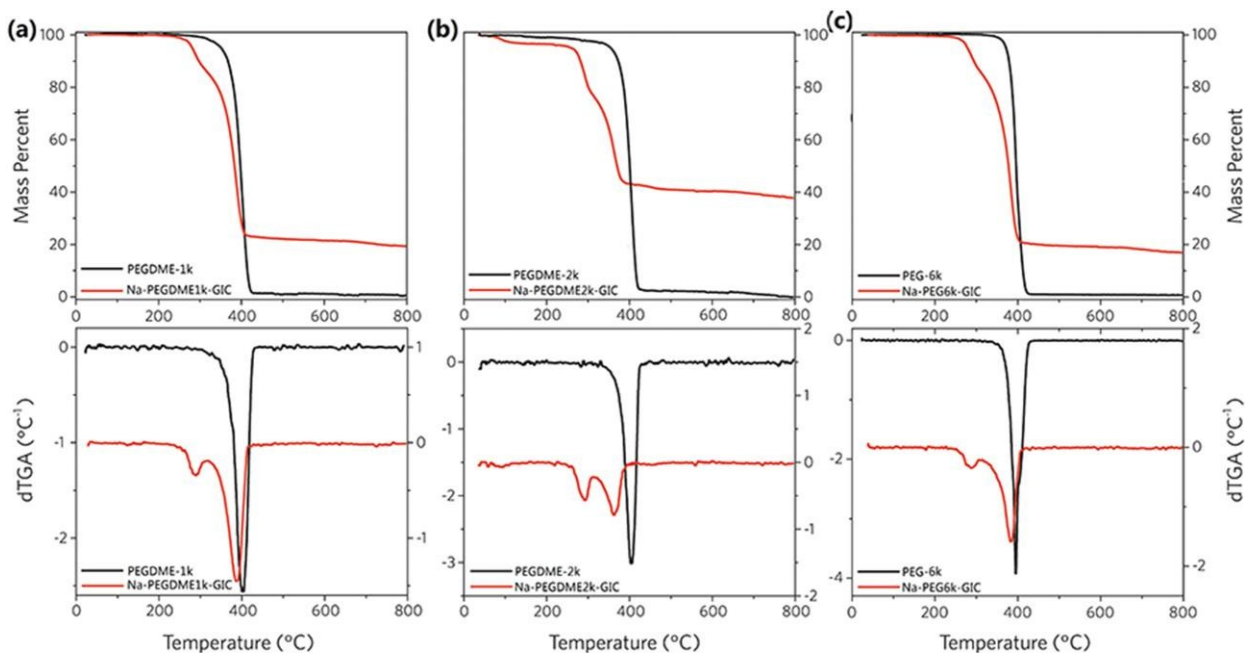
Fig. 5 Thermal analyses (TGA and derivative TGA plots) of Na-GIC products under N2 flow for reactions with PEGDME-1k, PEGDME-2k and PEG-6k. Each plot includes a trace for the starting polymer for comparison.

Nanoscale

Paper

Table 1 Structural and compositional data for synthesized GICs. All products were first stage, with single graphene sheets between polymer bilayers.

M	Co-intercalate	Δd / nm	Gallery type	Composition	Packing fraction	Domain size / nm
Na	DME	0.40	monolayer	N/A	N/A	N/A
Li	PEGDME-1k	0.81	bilayer	$[Li(CH_2CH_2O)_{3.4}]C_{25}$	0.32	37
Na	PEGDME-1k	0.83	bilayer	$[Na(CH_2CH_2O)_{2.6}]C_{13}$	0.49	37
K	PEGDME-1k	0.89	bilayer	$[K(CH_2CH_2O)_{2.6}]C_{11}$	0.52	27
Na	PEGDME-2k	0.83	bilayer	$[Na(CH_2CH_2O)_{1.4}]C_9$	0.40	39
Na	PEG-6k	0.84	bilayer	$[Na(CH_2CH_2O)_{2.4}]C_{10}$	0.60	30

products, a loss at temperature close to that with the native polymer (shown above), plus a lower-temperature loss at ≈250-320°C ascribed to degradation of the polymer co-intercalate in the GIC. Previous studies have shown a similar catalytic effect where intercalates and co-intercalates in GICs thermally degrade at reduced temperatures.[41, 42] The low-temperature peak areas were evaluated to determine co-intercalate contents in the GIC phase. Metal cation content was obtained by thermolysis under O_2 flow; above 800 °C all carbon is volatilized as CO_2 leaving only Li_2O, Na_2O or K_2O. The derived GIC compositions are shown in Table 1 (see ESI† Section 3 for details). By combining the compositions and GIC gallery expansions, gallery packing fractions of 0.41-0.60 were obtained (Table 1, and ESI† Section 4). From these results, GICs have similar gallery dimensions, but somewhat less densely packed polymer bilayers, than PEO nanocomposites with MPS_3 (packing fraction = 0.72-0.83),[6] or Na-montmorillonite (packing fraction = 0.68).[13]

Conclusions

Well-ordered GICs containing polyether intercalates are synthesized via direct reductive intercalation or co-intercalate exchange, providing new simple methods for generating nanocomposites comprising graphite and oligo or polyethers. The GIC products are first-stage and have intercalate bilayers and metal cations between reduced graphene sheets. If these GICs are applied as electrodes materials, these large Mw ether bilayers may remain within galleries and thus reduce the gallery volume changes required during charge/ discharge cycling.

Acknowledgements

Notes and references

1   M. M. Lerner, C. O. Oriakhi, Polymers in ordered nanocomposites, in: A. N. Goldstein (Ed.), Handbook of Nanophase Mateials, Marcel Dekker, Inc, New York, 1997, 199-219.
2   J. Wu and M. M. Lerner. *Chem. Mat.* 1993, **5**, 835-838.
3   X. Zhang, W. Yang and Y. Ma, *Electrochem. Solid-State Lett.,* 2009, **12**, A95-A98.
4   J. P. Lemmon and M. M. Lerner, *Chem. Mat.*, 1994, **6**, 207-210.
5   L. F. Nazar, H. Wu and W. P. Power, *J. Mater. Chem.*, 1995, **5**, 1985-1993.
6   A. U. Liyanage and M. M. Lerner, *RSC Adv.*, 2012, **2**, 474-479.
7   P. Maiti, K. Yamada, M. Okamoto, K. Ueda, K. Okamoto, *Chem. Mat.*, 2002, **14**, 4654-4661.
8   K. A. Carrado, P. Thiyagarajan and D. L. Elder, *Clays Clay Miner.* 1996, **44**, 506-514.
9   J. P. Lemmon and M. M. Lerner, *Solid State Commun.*, 1995, **94**, 533-537.
10 M. Alexandre and P. Dubois, *Mater. Sci. Eng. R Rep.*, 2000, **28**, 1-63.
11 C. -W. Chiu, T. -K. Huang, Y. -C. Wang, B. G. Alamani and J. -J. Lin, *Prog. Polym. Sci.*, 2014, **39**, 443-485.
12 A. B. Morgan and J. Gilman, *Mater. Matters*, 2007, **2**, 20-25.
13 A. U. Liyanage, E. U. Ikhuoria, A. A. Adenuga, V. T. Remcho and M. M. Lerner, *Inorg. Chem.*, 2013, **52**, 4603-4610.
14 B. P. Nair, C. Pavithran, J. D. Sudha and V. S. Prasad. *Langmuir,* 2010, **26**, 1431-1434.
15 V. Manríquez, P. Barahona, D. Ruiz and R. E. Avila, *Mater. Res. Bull.,* 2005, **40**, 475-483.
16 P. Meister, V. Siozios, J. Reiter, S. Klamor, S. Rothermel, O. Fromm, H.-W. Meyer, M. Winter and T. Placke, *Electrochim. Acta*, 2014, **130**, 625-633.
17 L.H. Huang, Z.H. Min and Q.Y. Zhang, *Rev. Adv. Mater. Sci.*, 2014, **36**, 13-20.
18 S. A. Solin, *Annu. Rev. Mater. Sci.,* 1997, **27**, 89-115.
19 S. A. Safran, *Solid State Phys.*, 1987, **40**, 183-246.
20 N. Daumas and A. Herold, *C. R. Acad. Sci. Paris Ser. C,* 1969, **268**, 373-375.
21 H. Podall, W. E. Foster and A. P. Giraitis, *J. Org. Chem.*, 1958, **23**, 82-85.
22 I. M. Panayotov and I. B. Rashkov, *Makromol. Chem.*, 1974, **175**, 3305-3307.
23 N. Akuzawa, *TANSO*, 2011, **248**, 96-101.
24 H. Shioyama, K. Tatsumi, N. Iwashita, K. Fujita and Y. Sawada, *Synth. Met.*, 1998, **96**, 229-233.
25 L. Sun, M. Xiao, J. Liu and K. Gong, *Eur. Polym. J.*, 2006, **42**, 259-264.
26 S. Stankovich, D. A. Dikin, O. C. Compton, G. H. B. Dommett, R. S. Ruoff and S. T. Nguyen, *Chem. Mater.,* 2010, **22**, 4153-4157.
27 Y. Matsuo, *Carbon*, 2014, **78**, 633.
28 H. Kim, A. A. Abdala and C. W. Macosko, *Macromol.*, 2010, **43**, 6515–6530.

Nanoscale Accepted Manuscript

29 T. Maluangnont, M. M. Lerner and K. Gotoh, *Inorg. Chem.*, 2011, **50**, 11676-11682.
30 W. Sirisaksoontorn and M. Lerner, *Inorg. Chem.*, 2013, **52**, 7139-7144.
31 G. Gokel, D. Goli and R. Schultz, *J. Org. Chem.*, 1983, **48**, 2837-2842.
32 Y. Mizutani, T. Abe, E. Ihara, K. Ikeda, M. Inaba, Z. Ogumi, T. Ohkubo, *TANSO*, 1997, **180**, 239-244.
33 Y. Mizutani, T. Abe, M. Inaba and Z. Ogumi, *Synth. Met.*, 2001, **125**, 153-159.
34 R. Setton, F. Béguin, L. Facchini, M. F. Quinton, A. P. Legrand, B. Ruisinger and H. Boehm, *J. Chem. Soc. Chem. Commun.*, 1983, 36-37.
35 B. Jache and P. Adelhelm, *Angew. Chem. Int. Ed.*, 2014, **53**, 10169-10173.
36 H. Kim, J. Hong, Y-U. Park, J. Kim, I. Hwang and K. Kang, *Adv. Funct. Mater.*, 2015, **25**, 534-541.
37 X. Zhang and M. M. Lerner, *Chem. Mater.*, 1999, **11**, 1100-1109.
38 A. Monshi, M. R. Foroughi and M. R. Monshi, *World J. Nano Sci. Eng.*, 2012, **2**, 154-160.
39 P. Co-Minh-Duc, C. Mai, R. Rivière and J. Golé, *J. Chim. Phys. Physicochim Biol.*, 1972, **69**, 991-995.
40 G. L. Doll, P. C. Eklund and J. E. Fischer, *Phys. Rev. B*, 1987, **36**, 4940-4945.
41 W. Sirisaksoontorn and M. M. Lerner, *ECS J. Solid State Sci. Technol.*, 2013, **2**, M28-M32.
42 N. Muradov, F. Smith and A. T-Raissi, *Catal. Today*, 2005, **102-103**, 225-233.

References in ESI
43 W. Luo, B. Wang, X. Wang, W. F. Stickle and X. Ji, *Chem. Commun.*, 2013, **49**, 10676-10678.
44 C. Sole, N. E. Drewetta and L. J. Hardwick, *Faraday Discuss.*, 2014, **172**, 223-237.
45 Y. H. Zhao, M. H. Abraham and A. M. Zissimos, *J. Org. Chem.*, 2003, **68**, 7368-7373.